

See discussions, stats, and author profiles for this publication at: <https://www.researchgate.net/publication/259253856>

Non-natural G-quadruplex in a non-natural environment

Article in *Photochemical and Photobiological Sciences* · December 2013

DOI: 10.1039/c3pp50199j · Source: PubMed

CITATIONS

5

READS

145

2 authors:



Shinaj K. Rajagopal

Indian Institute Of Science Education and Research, Thiruvananthapuram

10 PUBLICATIONS 185 CITATIONS

[SEE PROFILE](#)



Mahesh Hariharan

Indian Institute Of Science Education and Research, Thiruvananthapuram

112 PUBLICATIONS 2,716 CITATIONS

[SEE PROFILE](#)

Some of the authors of this publication are also working on these related projects:



NP-alkyl View project



Greek Cross(+) Aggregate View project

Non-natural G-quadruplex in a non-natural environment†‡

Shinaj K. Rajagopal and Mahesh Hariharan*

Cite this: *Photochem. Photobiol. Sci.*, 2014, **13**, 157

Received 29th June 2013,
Accepted 25th October 2013

DOI: 10.1039/c3pp50199j

www.rsc.org/pps

The biocompatibility as well as the sustainability of a deep eutectic solvent makes it a good substitute for aqueous media in studying biomolecules. Understanding the structure and stability of natural and non-natural G-quadruplexes in aqueous and highly viscous media will be useful in biological and nanodevice applications. We report the synthesis and conformational analysis of a model G-rich oligonucleotide G_3T_3 and non-natural G-rich sequences Pyr1–Pyr3 in aqueous and highly viscous media. Progressive increases in the loop replacement with a non-natural pyrene linker leads to a systematic increase of the thermal denaturation temperature of the modified G-rich oligonucleotides Pyr1–Pyr3 in 10 mM cacodylate buffer (pH 7.2) containing 100 mM KCl, as monitored using UV-Vis spectroscopy. A circular dichroism signal clearly revealed the formation of a predominantly anti-parallel vs. parallel conformation in the natural G-rich oligonucleotide G_3T_3 as well as the non-natural G-rich oligonucleotides Pyr1–Pyr3 in 10 mM cacodylate buffer (pH 7.2) containing 100 mM KCl. On the other hand, we observed thermodynamic destabilization of G-rich oligonucleotides in a deep eutectic solvent (DES; 1 : 2 choline chloride–urea) containing 100 mM KCl with an increase in loop replacements. Interestingly, we observed an exclusively parallel G-quadruplex conformation in the case of G_3T_3 in DES containing 100 mM KCl. While pyrene containing G-rich oligonucleotides Pyr1–Pyr3 exhibited a predominantly parallel vs. anti-parallel G-quadruplex conformation in DES containing 100 mM KCl.

Guanine rich oligonucleotides are prone to adopt stacks of planar G-quartets through Watson–Crick and Hoogsteen hydrogen bonding in the presence of metal ions.¹ G-quartet structures are widely spread in the genomic system and play a vital role in cellular processes such as replication,

recombination, transcription and translation.^{2–4} G-quartet based structures also have the potential to control the bottom-up synthesis of well-defined nanoarchitectures.⁵ Structure, stability⁶ and storage^{7,8} of G-quartet based structures in aqueous solution,^{9–11} room temperature ionic liquids (RTILs),¹² anhydrous deep eutectic solvent (DES)^{13,14} and a molecularly crowded polyethylene glycol (PEG) medium¹⁵ have been investigated in detail. While interest towards the stability of G-quadruplex structures in different non-natural environments is emerging, the stability of non-natural G-quadruplex structures both in natural and non-natural environments demands further attention. We report the synthesis and conformational analysis of a model G-rich oligonucleotide G_3T_3 and non-natural G-rich sequences Pyr1–Pyr3 (Fig. 1). A systematic replacement of lateral and diagonal thymine (TTT) containing loops from the model oligonucleotide G_3T_3 using a pyrene linker resulted in non-natural G-rich oligonucleotides Pyr1–Pyr3. Conformation and thermodynamic stability of modified G-rich oligonucleotides Pyr1–Pyr3 in comparison to the model G-rich oligonucleotide G_3T_3 is studied both in aqueous (cacodylate) buffer and a deep eutectic solvent (DES; 1 : 2 choline chloride–urea) medium. Incorporation of a fluorescent reporter^{15,16} such as a pyrene chromophore into the loop region of the G-rich sequence that possesses distinct

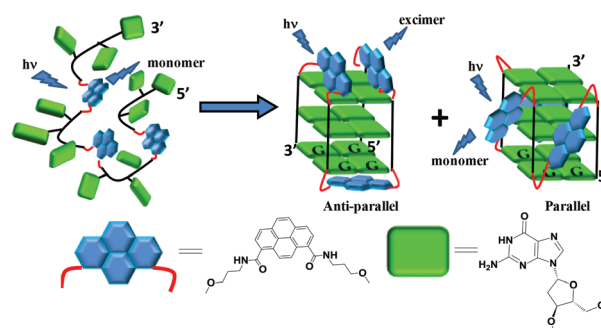


Fig. 1 Schematic representation of the intramolecular formation of a pyrene modified G-quadruplex and the structure of the pyrene linker and guanine.

School of Chemistry, Indian Institute of Science Education and Research
Thiruvananthapuram, CET Campus, Sreekaryam, Thiruvananthapuram, 695016
Kerala, India. E-mail: mahesh@iisertvm.ac.in

† Dedicated to the memory of Professor Nicholas J. Turro.

‡ Electronic supplementary information (ESI) available: Synthesis, characterisation of the pyrene linker and corresponding G-rich oligonucleotides, UV-Vis, CD, steady-state fluorescence data of oligonucleotides Pyr1–Pyr3. See DOI: 10.1039/c3pp50199j

Table 1 Sequence of G-rich oligonucleotides **Pyr1–Pyr3** and the model oligonucleotide (**G₃T₃**) used and the corresponding thermal denaturation temperatures (°C) under different conditions

Oligo	Sequence	T_m^a	T_m^b	T_m^c	T_m^d
G₃T₃	3'd(GGGTTTGGGTTTGGGTTTGGG)5'	70.2	—	68.8	—
Pyr1	3'd(GGG Pyr GGGTTTGGGTTTGGG)5'	69.9	69.7	60.9	30.4
Pyr2	3'd(GGG Pyr GGGTTTGGG Pyr GGG)5'	74.5	75.1	40.8	33.3
Pyr3	3'd(GGG Pyr GGG Pyr GGG Pyr GGG)5'	87.2	80.9	36.6	35.2

Measured in 10 mM sodium cacodylate buffer (pH 7.2) containing 100 mM KCl and monitored at ^a295 nm and ^b360 nm. Samples measured in DES containing 100 mM KCl monitored at ^c295 nm and ^d360 nm.

fluorescence behaviour (monomer *vs.* excimer) depending upon the conformation¹⁷ can provide insight on structural polymorphism. While end-labelled pyrene units^{18–21} in a G-rich sequence offer insight into conformational folding and un-folding, loop replacement in G-quadruplex structures can provide better structural information.

The pyrene linker (**Pyr**) is synthesized as per the procedure reported previously (Scheme S1, ESI†).²² Pyrene-1,8-dicarboxylic acid obtained from pyrene²³ is converted to the corresponding aminopropanol linker, followed by 4,4'-dimethoxytrityl protection on one hydroxyl and a phosphoramidite reaction on the other hydroxyl group to give the desired linker. Pyrene bisamide phosphoramidite is then incorporated into the G-rich oligonucleotides **Pyr1–Pyr3** (Table 1) through standard phosphoramidite chemistry.^{24,25} Further deprotection occurs using concentrated ammonium hydroxide, then purified using reverse phase HPLC and characterized by MALDI-TOF mass spectrometry (Table S1, ESI†). In order to understand the stability of natural and non-natural G-quadruplex sequences in a non-natural environment, we carried out measurements in deep eutectic solvent (DES; 1:2 choline chloride–urea) containing 100 mM KCl. We have prepared DES§ as per the procedure reported by Abbott and co-workers.²⁶

UV-Vis absorption spectra of pyrene incorporated G-rich oligonucleotides **Pyr1–Pyr3** in 10 mM sodium cacodylate buffer (pH 7.2) containing 100 mM KCl exhibited two distinct bands centered around 260 and 355 nm (Fig. 2A). While the absorption band centered around 260 nm corresponds to the electronic transitions in nucleobases, the broad band centered around 355 nm corresponds to the incorporated pyrene chromophore(s) in the G-rich sequences. A significant red shift of 10 nm corresponding to the pyrene chromophores in **Pyr1–Pyr3** when compared to the model pyrene derivative **Pyr** in 10 mM sodium cacodylate buffer (pH 7.2) containing 100 mM KCl clearly indicates the presence of π -stacking interactions between pyrene and the adjacent G-quartet (Fig. S1, ESI†). UV-Vis absorption spectra of **Pyr1–Pyr3** in deep eutectic solvent (DES; Fig. 2C) containing 100 mM KCl exhibited bands centered around 260 and 354 nm, similar to that in cacodylate buffer.

Upon excitation at 360 nm, **Pyr1** in 10 mM sodium cacodylate buffer containing 100 mM KCl exhibited an emission band centered around 397 nm corresponding to the

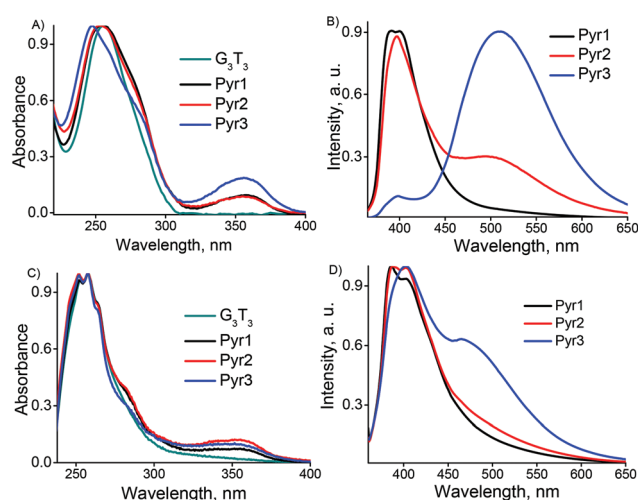


Fig. 2 Normalized absorption spectra of **G₃T₃**, **Pyr1**, **Pyr2** and **Pyr3** in (A) 10 mM sodium cacodylate buffer (pH 7.2) containing 100 mM KCl. (C) DES containing 100 mM KCl. Normalized fluorescence spectra of **Pyr1**, **Pyr2**, and **Pyr3** in (B) 10 mM sodium cacodylate buffer (pH 7.2) containing 100 mM KCl and (D) DES containing 100 mM KCl.

monomeric pyrene chromophore (Fig. 2B). While **Pyr2** and **Pyr3** under similar conditions exhibited two emission maxima centered around 397 and 500 nm (**Pyr2**)/510 nm (**Pyr3**) that correspond to monomer and excimer emissions of pyrene, respectively. The observed pyrene excimer emission in the case of **Pyr2** and **Pyr3** can arise from the ordered G-quadruplex structure resulting in cofacial π -stacking interactions between the pyrene units incorporated in the lateral loops. Moreover, incorporation of the pyrene linker **Pyr** in the diagonal loop of **Pyr3** seems to stabilise the G-quadruplex structure and results in better overlap of the pyrene units in the lateral loop. Enhanced overlap is consistent with the higher $I_{\text{excimer}}/I_{\text{monomer}}$ and larger red shift in the excimer emission for **Pyr3** (510 nm), when compared to **Pyr2** (500 nm). The relatively higher fluorescence intensity of excimer *vs.* monomer is a consequence of events such as (i) efficiency of photoinduced electron transfer between the constituents and (ii) the extent of overlap between the pyrene units. We attribute the enhanced ratio of excimer to monomer fluorescence intensity of **Pyr3** in cacodylate buffer in terms of the difference in efficacy of photoinduced electron transfer from guanine to the singlet excited state of pyrene ($\Delta G = 0.0 \pm 0.1$ V)²⁷ *vs.* excimeric pyrene, as reported by Lewis

and coworkers.²⁸ Excimeric pyrene could be less sensitive to fluorescence quenching by the G-stack, in agreement with the lower singlet state redox potentials of the pyrene excimer vs. monomer. Therefore we observe a strong quenching in the fluorescence intensity corresponding to monomeric pyrene when compared to excimeric pyrene in **Pyr3**.

Upon excitation at 360 nm, **Pyr1** in the deep eutectic solvent (DES; 1 : 2 choline chloride–urea) containing 100 mM KCl exhibited an emission band centered around 387 nm (Fig. 2D) corresponding to the monomeric pyrene chromophore, similar to that in cacodylate buffer. While **Pyr2** in deep eutectic solvent containing 100 mM KCl exhibited a predominant emission intensity at 387 nm, a weak broad shoulder around 460 nm is also observed. **Pyr3** under similar conditions exhibited two intense broad bands centered around 400 and 465 nm. The ratio of $I_{\text{excimer}}/I_{\text{monomer}}$ for **Pyr3** is found to be higher when compared to **Pyr2** in deep eutectic solvent. **Pyr2** and **Pyr3** have a lower ratio of $I_{\text{excimer}}/I_{\text{monomer}}$ in deep eutectic solvent when compared to that in cacodylate buffer. This clearly indicates that cacodylate buffer favours better overlap between the pyrene units in the lateral loop of **Pyr2** and **Pyr3** when compared to that in deep eutectic solvent containing 100 mM KCl.

With an increase in concentration of KCl, **Pyr2** in 10 mM sodium cacodylate buffer (pH 7.2) containing 100 mM KCl exhibited an evolution of strong CD signal centered at 260 and 290 nm (1 : 1.1) that corresponds to parallel and anti-parallel G-quadruplex structures respectively (Fig. S2, ESI[†]). A similar trend was observed for **Pyr1** (1 : 1.7) and **Pyr3** (1 : 1.7) that supports the formation of parallel and anti-parallel G-quadruplex structures (Fig. 3A). Similarly, the model G-rich oligonucleotide (G_3T_3) in 10 mM sodium cacodylate buffer (pH 7.2) containing 100 mM KCl exhibited CD signal centered at 260 and 290 nm having an intensity ratio of 1 : 2.4 that corresponds to parallel and anti-parallel G-quadruplex structures.^{29–32} On the other hand, **Pyr1** in DES medium containing 100 mM KCl exhibited two CD signals centered at 260 and 290 nm with a ratio of 1 : 0.6. Observation of CD signals at 260 and 290 nm (Fig. 3B) indicates the existence of a combination of parallel and anti-parallel G-quadruplex structures, respectively. **Pyr2** in DES medium exhibited a moderate increase in the population of parallel vs. anti-parallel G-quadruplex structures (1 : 0.5) when compared to **Pyr1**. **Pyr3** under similar conditions

exhibited a predominant formation of parallel vs. anti-parallel G-quadruplex structures (1 : 0.15). The model G-rich oligonucleotide (G_3T_3) in DES medium containing 100 mM KCl showed a CD signal at 260 nm suggesting the existence of a parallel G-quadruplex structure.¹³

The observed higher $I_{\text{excimer}}/I_{\text{monomer}}$, larger red-shift in the excimer emission maximum and the existence of an anti-parallel G-quadruplex structure in 10 mM sodium cacodylate buffer containing 100 mM KCl clearly indicates the fact that an anti-parallel structure favours excimer emission of pyrene in **Pyr2–Pyr3**. While the decrease in excimer emission corresponding to the pyrene chromophore in **Pyr2** and **Pyr3** indicates the formation of a parallel structure that has pyrene units propelled out of the G-quadruplex disfavours the orbital overlap between the pyrene units. However, the observed moderate excimer emission corresponding to the pyrene chromophore in **Pyr2** and **Pyr3** could be attributed to a minor population of an anti-parallel structure, as evidenced from the circular dichroism signal.

With an increase in temperature, **Pyr1** in 10 mM sodium cacodylate buffer containing 100 mM KCl exhibited a sigmoidal change having a thermal denaturation temperature (T_m) of 69.9 °C (Table 1) when monitored at 295 nm by an UV-Vis absorption method (Fig. 4A). The observed strong hypochromism (50%) and sigmoidal transition in the case of **Pyr1** in 10 mM sodium cacodylate buffer containing 100 mM KCl strongly suggests the formation of a G-quadruplex structure.³³ We observed a similar T_m value of 70.2 °C for the model G-rich oligonucleotide (G_3T_3) in 10 mM sodium cacodylate buffer containing 100 mM KCl. **Pyr2** under similar conditions exhibited an increase in the melting temperature ($T_m = 74.5$ °C) possibly due to the two lateral loop replacements when compared to a single lateral loop replacement in **Pyr1**. A significant increase in melting temperature ($T_m = 87.2$ °C) was observed for **Pyr3** that has thymine–thymine–thymine (TTT) steps replaced by the **Pyr** linker in both the lateral loops and the diagonal loop. A remarkable increase in the T_m value of **Pyr3** is consistent with the enhanced pyrene excimer emission arising from favourable overlap of pyrene units in the lateral loops as a consequence of diagonal loop replacement by the **Pyr** linker. The thermal denaturation temperature monitored at the pyrene region (360 nm) exhibited an increase with the increase in number of **Pyr** linker replacements, in good agreement with the T_m value monitored at 295 nm.

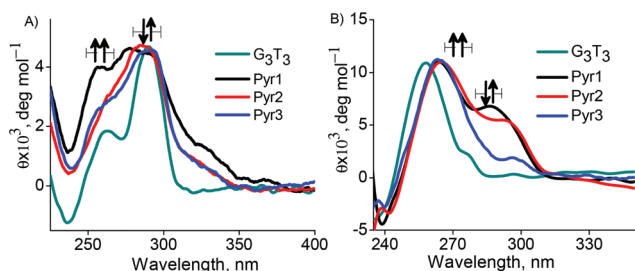


Fig. 3 Circular dichroism spectra of G_3T_3 , **Pyr1**, **Pyr2** and **Pyr3** in (A) 10 mM sodium cacodylate buffer (pH 7.2) containing 100 mM KCl and (B) in DES containing 100 mM KCl.

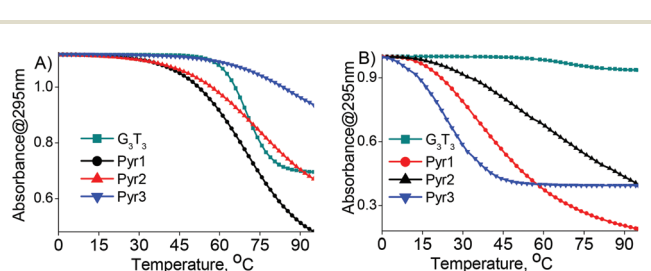


Fig. 4 Normalized UV melting spectra of G_3T_3 , **Pyr1**, **Pyr2** and **Pyr3** in (A) 10 mM sodium cacodylate buffer (pH 7.2) containing 100 mM KCl and (B) in DES containing 100 mM KCl.

Similar thermal denaturation profiles were observed at 295 and 360 nm for G-rich sequences such as **Pyr1** and **Pyr2** in 10 mM sodium cacodylate buffer (pH 7.2) containing 100 mM KCl where the G-quadruplex tetrad melts simultaneously with the unstacking between the **Pyr** and the G-stack. While in **Pyr1** and **Pyr2** in DES containing 100 mM KCl and **Pyr3** in cacodylate buffer, unstacking of **Pyr** precedes the melting of the G-stack. Detailed thermodynamic/computational analysis on the observed discrimination in the unstacking between the pyrene chromophore and the G-stack vs. quadruplex melting in pyrene containing G-rich sequences is in progress in our laboratory.

In DES medium containing 100 mM KCl, the model G-rich oligonucleotide (G_3T_3) exhibited a T_m value of 68.8 °C, comparable to that in cacodylate buffer (Fig. 4B). With an increase in the number of **Pyr** linker replacements, we observed a systematic decrease in the T_m value that resulted in 36.6 °C for **Pyr3**, in contrast to that in the case of cacodylate buffer. Thermal denaturation monitored at the pyrene chromophore region showed a relatively lower dissociation temperature indicating a weak interaction between pyrene and the G-quartet, in the case of **Pyr1–Pyr3** in DES medium.

Human telomeric DNA (Htelo) shows both the parallel and anti-parallel conformations under physiological conditions. Htelo adopts an exclusively parallel stranded conformation in physiological K^+ solution under molecular crowding conditions created by 40% PEG (polyethylene glycol), as reported earlier by Tan and coworkers.¹⁵ Experiments in non-natural environments were further extended to a water free medium (DES; deep eutectic solvent) by Hud and coworkers.¹³ As confirmed through circular dichroism studies, Htelo in DES exhibits a parallel stranded conformation consistent with Htelo in 40% PEG solution. While interest towards the stability of G-quadruplex structures in different non-natural environments is emerging, the stability of non-telomeric and non-natural G-quadruplex structures both in natural and non-natural environments demands further attention. Our study on the non-telomeric G-rich sequence G_3T_3 reveals a combination of parallel and anti-parallel conformations in cacodylate buffer, consistent with Htelo. In a highly viscous anhydrous deep eutectic solvent (DES) medium, G_3T_3 showed only a parallel conformation similar to Htelo in DES medium. Non-natural G-rich sequences **Pyr1–Pyr3** having the TTT loop(s) replaced by pyrene-linkers display a mixture of parallel and antiparallel stranded conformations both in natural and DES media. The existence of an anti-parallel conformation, one of the more commonly occurring conformations in physiological media, in **Pyr1–Pyr3** in a non-natural medium allows us to investigate the stability in a water free environment.

Conclusions

In summary, we report the contrasting behaviours of non-natural G-quadruplex geometry in natural (cacodylate buffer) and non-natural (DES) media, when compared to a natural

G-quadruplex geometry under similar conditions. The natural G-rich sequence G_3T_3 exhibits a combination of parallel and anti-parallel conformations in cacodylate buffer, while in a highly viscous anhydrous deep eutectic solvent (DES) medium only parallel conformation of G_3T_3 was observed. We observed a similar combination of parallel and anti-parallel G-quadruplex formation in pyrene incorporated G-rich oligonucleotides **Pyr1–Pyr3** in cacodylate buffer as well as DES medium. Such modified G-quadruplex structures with attractive thermodynamic properties could have uses in biological and nanodevice applications. Moreover, chromophore labelled G-quadruplex structures in water free environments such as a DES medium could provide an insight into the role of water molecules in the photoinduced excited state processes of quadruplex structures.

Acknowledgements

Financial support from the Science and Engineering Research Board, INDIA (SERB/F/0962) is gratefully acknowledged.

Notes and references

§Karl-Fischer analysis exhibited only trace amounts ($<0.24 \pm 0.03\%$) of water present in the DES medium.

- 1 *Quadruplex nucleic acids*, ed. S. Neidle and S. Balasubramanian, Royal Society of Chemistry, Cambridge, UK, 2006.
- 2 J. E. Johnson, J. S. Smith, M. L. Kozak and F. B. Johnson, In vivo veritas: Using yeast to probe the biological functions of G-quadruplexes, *Biochimie*, 2008, **90**, 1250–1263.
- 3 E. Henderson, C. C. Hardin, S. K. Walk, I. Tinoco Jr. and E. H. Blackburn, Telomeric DNA oligonucleotides form novel intramolecular structures containing guanine-guanine base pairs, *Cell*, 1987, **51**, 899–908.
- 4 T. von Zglinicki, Telomeres, telomerase and the cancer cell: An introduction, *Cancer Lett.*, 2003, **194**, 137–138.
- 5 S. Lena, S. Masiero, S. Pieraccini and G. P. Spada, Guanine hydrogen-bonded scaffolds: A new way to control the bottom-up realisation of well-defined nanoarchitectures, *Chem.–Eur. J.*, 2009, **15**, 7792–7806.
- 6 H. Tateishi-Karimata and N. Sugimoto, A–T base pairs are more stable than G–C base pairs in a hydrated ionic liquid, *Angew. Chem., Int. Ed.*, 2011, **51**, 1416–1419.
- 7 R. Vijayaraghavan, A. Izgorodin, V. Ganesh, M. Surianarayanan and D. R. MacFarlane, Long-term structural and chemical stability of DNA in hydrated ionic liquids, *Angew. Chem., Int. Ed.*, 2010, **49**, 1631–1633.
- 8 K. Fujita, D. R. MacFarlane and M. Forsyth, Protein solubilising and stabilising ionic liquids, *Chem. Commun.*, 2005, 4804–4806.
- 9 P. Balagurumoorthy and S. K. Brahmachari, Structure and stability of human telomeric sequence, *J. Biol. Chem.*, 1994, **269**, 21858–21869.

- 10 P. Hazel, J. Huppert, S. Balasubramanian and S. Neidle, Loop-length-dependent folding of G-quadruplexes, *J. Am. Chem. Soc.*, 2004, **126**, 16405–16415.
- 11 S. Amrane, R. W. L. Ang, Z. M. Tan, C. Li, J. K. C. Lim, J. M. W. Lim, K. W. Lim and A. T. Phan, A novel chair-type G-quadruplex formed by a bombyx mori telomeric sequence, *Nucleic Acids Res.*, 2009, **37**, 931–938.
- 12 K. Fujita and H. Ohno, Stable G-quadruplex structure in a hydrated ion pair: Cholinium cation and dihydrogen phosphate anion, *Chem. Commun.*, 2012, **48**, 5751–5753.
- 13 F. M. Lannan, I. Mamajanov and N. V. Hud, Human telomere sequence DNA in water-free and high-viscosity solvents: G-quadruplex folding governed by kramers rate theory, *J. Am. Chem. Soc.*, 2012, **134**, 15324–15330.
- 14 I. Mamajanov, A. E. Engelhart, H. D. Bean and N. V. Hud, DNA and rna in anhydrous media: Duplex, triplex, and G-quadruplex secondary structures in a deep eutectic solvent, *Angew. Chem., Int. Ed.*, 2010, **122**, 6454–6458.
- 15 Y. Xue, Z.-Y. Kan, Q. Wang, Y. Yao, J. Liu, Y.-H. Hao and Z. Tan, Human telomeric DNA forms parallel-stranded intramolecular G-quadruplex in K⁺ solution under molecular crowding condition, *J. Am. Chem. Soc.*, 2007, **129**, 11185–11191.
- 16 A. Nadler, J. Strohmeier and U. Diederichsen, 8-vinyl-2'-deoxyguanosine as a fluorescent 2'-deoxyguanosine mimic for investigating DNA hybridization and topology, *Angew. Chem., Int. Ed.*, 2011, **50**, 5392–5396.
- 17 A. Tsuchida, T. Ikawa, T. Tomie and M. Yamamoto, Intramolecular pyrene excimer formation of 1,3-dipyrenylpropanes with full and partial ring overlaps, *J. Phys. Chem.*, 1995, **99**, 8196–8199.
- 18 S. Nagatoishi, T. Nojima, B. Juskowiak and S. Takenaka, A pyrene-labeled G-quadruplex oligonucleotide as a fluorescent probe for potassium ion detection in biological applications, *Angew. Chem., Int. Ed.*, 2005, **44**, 5067–5070.
- 19 H. Zhu and F. D. Lewis, Pyrene excimer fluorescence as a probe for parallel G-quadruplex formation, *Bioconjugate Chem.*, 2007, **18**, 1213–1217.
- 20 D. Margulies and A. D. Hamilton, Protein recognition by an ensemble of fluorescent DNA G-quadruplexes, *Angew. Chem., Int. Ed.*, 2009, **48**, 1771–1774.
- 21 Y. J. Seo, I. J. Lee, J. W. Yi and B. H. Kim, Probing the stable G-quadruplex transition using quencher-free end-stacking ethynyl pyrene-adenosine, *Chem. Commun.*, 2007, 2817–2819.
- 22 S. M. Langenegger and R. Haner, Excimer formation by interstrand stacked pyrenes, *Chem. Commun.*, 2004, 2792–2793.
- 23 H. Vollmann, H. Becker, M. Corell and H. Streeck, Beiträge zur kenntnis des pyrens und seiner derivat, *Justus Liebigs Ann. Chem.*, 1937, **531**, 1–159.
- 24 R. L. Letsinger and T. Wu, Use of a stilbenedicarboxamide bridge in stabilizing, monitoring, and photochemically altering folded conformations of oligonucleotides, *J. Am. Chem. Soc.*, 1995, **117**, 7323–7328.
- 25 R. T. Cheriya, J. Joy, S. K. Rajagopal, K. Nagarajan and M. Hariharan, DNA-enforced conformational restriction of an atropisomer, *J. Phys. Chem. C*, 2012, **116**, 22631–22636.
- 26 A. P. Abbott, G. Capper, D. L. Davies, R. K. Rasheed and V. Tambyrajah, Novel solvent properties of choline chloride/urea mixtures, *Chem. Commun.*, 2003, 70–71.
- 27 K. Siegmund, P. Daublain, Q. Wang, A. Trifonov, T. Fiebig and F. D. Lewis, Structure and photoinduced electron transfer in DNA hairpin conjugates possessing a tethered 5'-pyrenecarboxamide, *J. Phys. Chem. B*, 2009, **113**, 16276–16284.
- 28 F. D. Lewis, Y. Zhang and R. L. Letsinger, Bispyrenyl excimer fluorescence: A sensitive oligonucleotide probe, *J. Am. Chem. Soc.*, 1997, **119**, 5451–5452.
- 29 N. Smargiasso, F. Rosu, W. Hsia, P. Colson, E. S. Baker, M. T. Bowers, E. De Pauw and V. Gabelica, G-quadruplex DNA assemblies: Loop length, cation identity, and multimer formation, *J. Am. Chem. Soc.*, 2008, **130**, 10208–10216.
- 30 T. Fujimoto, D. Miyoshi, H. Tateishi-Karimata and N. Sugimoto, Thermal stability and hydration state of DNA G-quadruplex regulated by loop regions, *Nucleic Acids Symp. Ser.*, 2009, **53**, 237–238.
- 31 A. Arora and S. Maiti, Stability and molecular recognition of quadruplexes with different loop length in the absence and presence of molecular crowding agents, *J. Phys. Chem. B*, 2009, **113**, 8784–8792.
- 32 A. Guédin, P. Alberti and J.-L. Mergny, Stability of intramolecular quadruplexes: Sequence effects in the central loop, *Nucleic Acids Res.*, 2009, 1–9.
- 33 J.-L. Mergny, A.-T. Phan and L. Lacroix, Following G-quartet formation by UV-spectroscopy, *FEBS Lett.*, 1998, **435**, 74–78.